High-temperature sensors for NO and NO_2 based on stabilized zirconia and spinel-type oxide electrodes

Geyu Lu, Norio Miura and Noboru Yamazoe*

Department of Materials Science and Technology, Graduate School of Engineering Sciences, Kyushu University, Kasuga-shi, Fukuoka 816, Japan

Zirconia-based electrochemical devices attached with an oxide sensing electrode have been examined for gas sensing properties towards NO and NO_2 at high temperature. Among the twelve kinds of spinel-type oxides tested, $CdCr_2O_4$ was the most sensitive electrode material to both NO and NO_2 in air at 500–600 °C, also being endowed with quick response and recovery characteristics. Values of E_{EMF} of the $CdCr_2O_4$-attached device decreased or increased linearly with an increase in the logarithm of NO or NO_2 concentration, respectively. The same device gave small or insignificant cross-sensitivities to H_2, CO, CH_4, CO_2 and H_2O. Sensing mechanisms involving mixed potential were confirmed from the measurements of polarization curves.

Solid-state gas sensors to detect NO and NO_2 (abbreviated NO_x) have been demanded for monitoring and controlling exhausts from automobiles. The sensors are required to be able to work at high temperatures of *ca.* 500 °C and above. So far, several solid-state NO_x sensors have been reported, *e.g.*, conductometric sensors using semiconducting WO_3[1–3] and potentiometric and amperometric sensors[4–8] using a solid electrolyte/auxiliary phase couple such as NASICON (Na^+ super ionic conductor)/sodium nitrite. These devices show good response behaviour especially to NO_2 at relatively low temperatures of 200–300 °C, but at the high temperatures required for the automobile emission control they lose sensitivity or are simply unable to work. Recently, we have reported a possibility of developing new types of solid-electrolyte gas sensors by introducing oxide electrodes. It has been demonstrated that the devices combining stabilized zirconia with WO_3,[9] $CdMn_2O_4$[10,11] and ZnO[12,13] exhibited promising sensing performance towards H_2S, NO_x and H_2, respectively, at fairly high temperatures. The sensing mechanisms of these devices are based on the mixed potential generated at the oxide sensing electrodes, so that the selection of a proper oxide electrode is critically important for the sensing performance. As for sensing NO_x, our search for electrode oxides has revealed that, among the various single-metal oxides tested, CdO and Mn_2O_3 are effective for detecting NO_2 and NO, respectively. Remarkably a mixed-metal oxide consisting of these constituents, $CdMn_2O_4$, has been shown to exhibit better sensing performance towards both NO and NO_2 at 500–600 °C. This fact suggests the importance of extending the search for electrode materials to include various mixed-metal oxides.

Here, we focused attention on twelve kinds of spinel-type oxides derived from trivalent transition metals (Co, Fe, Mn and Cr) and divalent transition metals (Cu, Zn and Cd). Each oxide was attached to stabilized zirconia as an oxide electrode and the resulting device was examined for NO or NO_2 sensing properties at temperatures of 500–600 °C. The device attached with the $CdCr_2O_4$ electrode which exhibited the best sensing properties was further subjected to detailed performance tests as well as electrochemical measurements in relation to the NO_x sensing mechanism.

Experimental

Spinel-type oxides were prepared from the mixtures of constituent metal nitrates by calcination at 800–900 °C for 5 h in air. Formation of single-phase spinel-type oxides was confirmed by X-ray diffraction analysis. Sensor devices were fabricated by using a half-open yttria-stabilized zirconia tube (YSZ, 8 mol% Y_2O_3 doped, NKT), of length 30 cm, and 5 and 8 mm in inner and outer diameter, respectively, as shown in Fig. 1. Pt paste was applied to the outside of the bottom of the tube, and was calcined at 1200 °C for 30 min. The Pt layer thus formed was porous and *ca.* 30 μm thick. The powder of each spinel-type oxide was applied on top of this as a paste mixed with α-terpineol and ethyl cellulose. Upon calcination at 700 °C for 2 h, a porous oxide layer *ca.* 30 μm thick was obtained which served as the sensing electrode. As a reference (or counter) electrode, Pt black was placed and fixed mechanically with a Pt mesh on the inside of the bottom of the tube.

Gas sensing properties were measured in a conventional gas-flow apparatus equipped with a heating facility. Sample gases containing various concentrations of NO or NO_2 in air were prepared by mixing each gas, 1000 ppm (μl l^{-1}) NO in N_2 or 200 ppm NO_2 in air, with dry synthetic air and/or O_2. With the reference electrode always being exposed to static atmospheric air, the gas flow (100 cm^3 min^{-1}) over the sensing electrode was switched between synthetic air and the sample gases. Electromotive force values (E_{EMF} of the device was measured with a digital electrometer (Advantest, TR8652). Polarization curves were measured by controlling the sensing electrode potential with a potentiostat (Hokuto Denko, HA-101), referring to the reference Pt electrode.

Results and Discussion

NO_x sensing characteristics

Twelve spinel-type oxides were examined for sensing electrode properties upon attachment to zirconia-based devices. Fig. 2

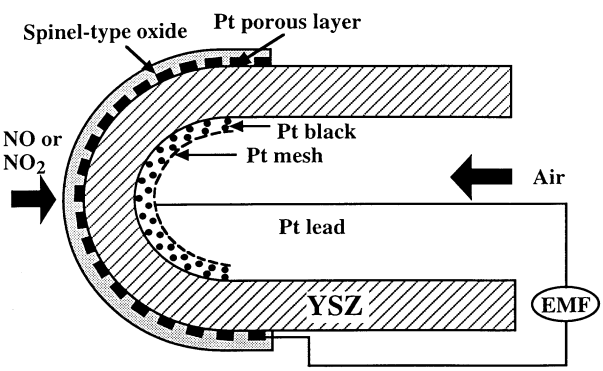

Fig. 1 Schematic view of a stabilized zirconia-based electrochemical device attached to an oxide electrode

Table 1 Comparison between mixed potentials estimated E_{EMF} and values observed for the $CdCr_2O_4$-attached device at 550 °C

NO_x (conc/ppm)	mixed potential/mV (estimated)	E_{EMF}/mV (observed)
NO_2 (80)	27	25
NO_2 (200)	45	44
NO (200)	−15	−15
NO (600)	−25	−26

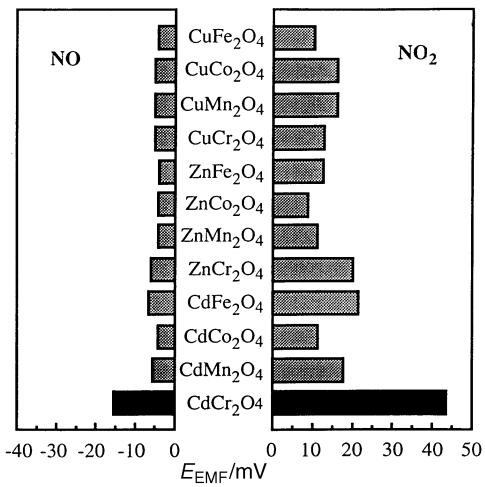

Fig. 2 E_{EMF} values of various oxide-attached devices to NO and NO_2, each 200 ppm in air, at 550 °C

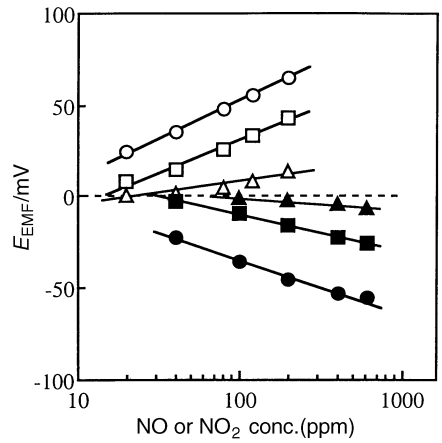

Fig. 3 Dependence of E_{EMF} on the logarithm of the NO (filled symbols) and NO_2 (open symbols) concentration for the device attached with $CdCr_2O_4$ at 500 (○, ●), 550 (□, ■) and 600 °C (△, ▲)

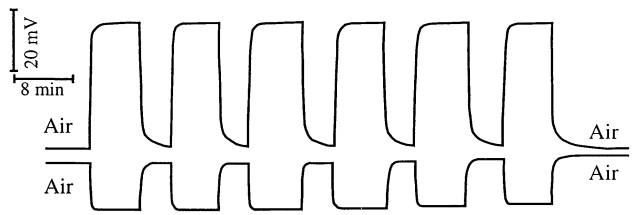

Fig. 4 Response transients of a $CdCr_2O_4$-attached device on switching on and off to 200 ppm NO (lower) or NO_2 (upper) at 550 °C

shows E_{EMF} values of oxide-attached devices upon exposure to NO and NO_2, each 200 ppm in air, at 550 °C. In the absence of NO_x, E_{EMF} was close to zero so that the E_{EMF} values can be regarded as the responses to NO and NO_2. The E_{EMF} values were strongly dependent on the oxides and the gases tested. Characteristically the direction of the E_{EMF} response was negative and positive on exposure to NO and NO_2, respectively. It was also characteristic that, for a given oxide, the E_{EMF} response to NO_2 was always larger in magnitude than that to NO. Among the oxides tested, $CdCr_2O_4$ gave the largest response to both NO and NO_2, with many other spinel-type oxides showing sensitivities to NO_x comparable to those of $CdMn_2O_4$. We reported previously that $CdMn_2O_4$ was far more sensitive to NO_x than various single-metal oxides.[10,11] These data may suggest that either the spinel structure or the fact that the materials are complex oxides is advantageous for sensitivity towards NO_x. Since the device using the $CdCr_2O_4$ electrode was the most sensitive it was subjected to more detailed investigations.

Fig. 3 shows E_{EMF} values of the $CdCr_2O_4$-attached device as a function of NO or NO_2 concentration at 500, 550 and 600 °C. Values of E_{EMF} were almost linear with the logarithm of concentration at each temperature tested. As the temperature increased, the response as well as its concentration dependence (slope) decreased. At 500 °C, E_{EMF} was −55 and 65 mV to 200 ppm NO and 200 ppm NO_2, respectively, and their concentration dependence (slope) was −29 and 40 mV (decade)$^{-1}$ for NO and NO_2, respectively. As extrapolated from the E_{EMF} *vs.* concentration correlations, the lower detection limits of the device would be *ca.* 6 or 20 ppm for NO_2 and 7 or 30 ppm for NO at 500 and 550 °C, respectively. These values seem to be fairly attractive as judged from the car emission standards now adopted, although the operating temperature of 500 or 550 °C would not always be high enough for practical applications.

Fig. 4 shows the response transients of the same device to turning on and off NO and NO_2, both 200 ppm in air, repeatedly at 550 °C. The response and recovery were fairly rapid and very well reproduced in the six successive runs tested. The cross-sensitivities of the device to H_2 (200 ppm), CO (200 ppm), CH_4 (200 ppm) and CO_2 (2000 ppm) were also tested at 550 °C. As summarized in Fig. 5, the cross-sensitivities obtained were far smaller than the sensitivities towards NO and NO_2. Fig. 6 shows the variation of E_{EMF} to various concentrations of NO_2 in the presence or absence of water vapour (233 Pa) at 550 °C; as shown, the NO_2 sensing characteristics were scarcely affected by the presence of water vapour.

Given such resistance to interference by coexistent gases as well as the fairly good sensing characteristics, the $CdCr_2O_4$-attached device appears to be promising as a sensor for NO or NO_2 operative at fairly high temperature. Unfortunately, however, this device can not be applied to a mixture of NO and NO_2, because of the widely different sensing properties towards the gases. Nevertheless, the detection of total NO_x would be possible if the mixture were to be converted to either NO or NO_2 prior to contact with the device.

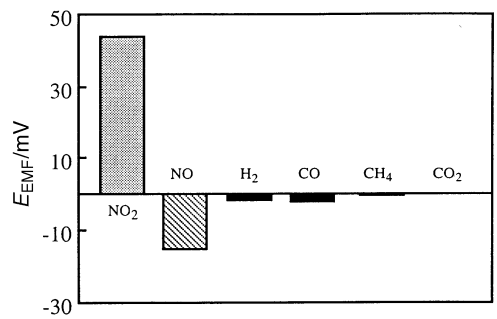

Fig. 5 Sensitivity of a $CdCr_2O_4$-attached device to various gases (200 ppm, except for CH_4 and CO_2: 2000 ppm) at 550 °C

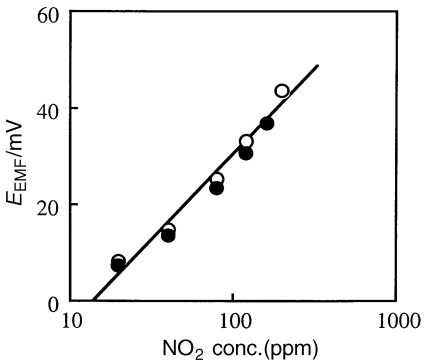

Fig. 6 Dependence of E_{EMF} on NO_2 concentration for a $CdCr_2O_4$-attached device in the presence (●) and absence (○) of water vapour (233 Pa) at 550 °C

Sensing mechanism

The present sensing device has the following electrochemical cell structure:

$$\text{air, Pt|YSZ|Pt,}CdCr_2O_4\text{, }NO_x\text{ (+air)}$$

The left-hand side of the cell is an oxygen-sensitive half-cell, in which the following reaction of oxygen proceeds.

$$O_2 + 4e^- \rightleftharpoons 2O^{2-} \quad (1)$$

In air (21 vol.% oxygen), the electrode potential of this half-cell is fixed. The right-hand side of the cell acts as a half-cell, the electrode potential of which is dependent on the NO or NO_2 concentration. To account for the NO_x-sensitive nature of this half-cell, one should consider the structure of the YSZ/electrode interface. Although the Pt layer is in contact with YSZ in the device, it does not seem to work as a sensing electrode, since the device without being attached with the oxide does not generate a significant E_{EMF} upon exposure to NO_x at 500 °C or above. In the presence of O_2 and NO_x, cathodic and anodic reactions can proceed simultaneously at the YSZ/electrode interface of the half-cell. It is considered that some of the oxide particles deposited have penetrated through pores of the Pt layer to contact directly with the YSZ electrolyte and it is tentatively assumed that the resulting YSZ/oxide interface is responsible for NO_x sensing while the Pt layer acts merely as an electronic probe in equilibrium with the oxide.

It is reasonable to assume that NO and NO_2 combine with or dissociate oxygen electrochemically, respectively, at the YSZ/oxide interface. In the presence of O_2, each reaction can combine with the electrochemical reaction of oxygen. For NO_2, a cathodic reaction of NO_2 combines with the anodic reaction of O_2 as follows.

$$NO_2 + 2e^- \rightarrow NO + O^{2-} \quad (2)$$

$$2O^{2-} \rightarrow O_2 + 4e^- \quad (3)$$

As a result, the electrode potential shifts upward to a mixed potential. In the case of NO, on the other hand, electrochemical reactions (4) and (5) form a local cell, resulting in a downward shift of the electrode potential.

$$O_2 + 4e^- \rightarrow 2O^{2-} \quad (4)$$

$$NO + O^{2-} \rightarrow NO_2 + 2e^- \quad (5)$$

These mixed potentials can be treated quantitatively, as has already been done for H_2S[9] and H_2 sensors.[13] For an NO_2–O_2 mixture, the cathodic and anodic current densities for reactions (2) and (3) should be given by the following general expressions, respectively, where the anodic current is taken to be positive.

$$i_{NO_2} = -i^0_{NO_2} \exp\{-2\alpha_1 F(E - E^0_{NO_2})/RT\} \quad (I)$$

$$i_{O_2} = i^0_{O_2} \exp\{4\alpha_2 F(E - E^0_{O_2})/RT\} \quad (II)$$

Here, E is the electrode potential, E^0 the electrode potential at equilibrium, i^0 the exchange current density and α the transfer coefficient; F, R and T have the usual meanings. The exchange current densities can be assumed to obey the following kinetic equations.

$$i^0_{NO_2} = B_1 C^m_{NO_2} \quad (III)$$

$$i^0_{O_2} = B_2 C^n_{O_2} \quad (IV)$$

Here, C is the concentration of NO_2 or O_2, and B_1, B_2, m and n are constants. The mixed potential E_M is defined as the electrode potential at which $|i_{NO_2}| = |i_{O_2}|$ or $i_{NO_2} + i_{O_2} = 0$. By combining this condition with eqn. (I)–(IV), E_M can be expressed by

$$E_M = E_0 + mA \ln C_{NO_2} - nA \ln C_{O_2} \quad (V)$$

where E_0 and A are

$$E_0 = \frac{RT}{(2\alpha_1 + 4\alpha_2)F} \ln(B_1/B_2) + \frac{\alpha_1 E^0_{NO_2} + 2\alpha_2 E^0_{O_2}}{(\alpha_1 + 2\alpha_2)} \quad (VI)$$

$$A = \frac{RT}{(2\alpha_1 + 4\alpha_2)F} \quad (VII)$$

Treatment of an NO–O_2 mixture is also straightforward. The cathodic and anodic current densities as well as the exchange current densities for reactions (4) and (5) are expressed as follows.

$$i_{O_2} = -i^0_{O_2} \exp\{-4\alpha_3 F(E - E^0_{O_2})\} \quad (VIII)$$

$$i_{NO} = i^0_{NO} \exp\{2\alpha_4 F(E - E^0_{NO})\} \quad (IX)$$

$$i^0_{O_2} = B_3 C^p_{O_2} \quad (X)$$

$$i^0_{NO} = B_4 C^q_{NO} \quad (XI)$$

The mixed potential is now given by

$$E_M = E_0 + pA \ln C_{O_2} - qA \ln C_{NO} \quad (XII)$$

where

$$E_0 = \frac{RT}{(4\alpha_3 + 2\alpha_4)F} \ln(B_3/B_4) + \frac{2\alpha_3 E^0_{O_2} + \alpha_4 E^0_{NO}}{(2\alpha_3 + \alpha_4)} \quad (XIII)$$

$$A = \frac{RT}{(4\alpha_3 + 2\alpha_4)F} \quad (XIV)$$

The symbols used in eqn. (VIII)–(XIV) have the same meanings as used in eqn. (I)–(VII).

Eqn. (V) and (XII) indicate that, when C_{O_2} is fixed, the mixed potential should increase or decrease linearly with an increase in the logarithm of C_{NO_2} or C_{NO}, in agreement with what was observed experimentally (Fig. 4). Under the condition of fixed concentration of NO or NO_2, on the other hand, E_M should go down or up linearly with the logarithm of concentration of O_2. Fig. 7 shows the E_{EMF} *vs.* O_2 concentration

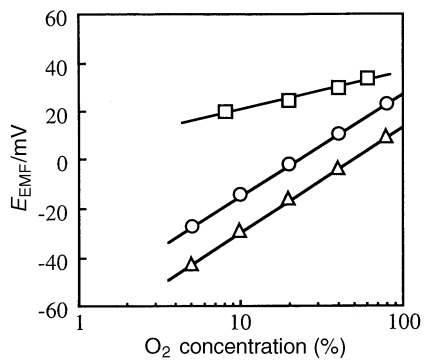

Fig. 7 Correlations between E_{EMF} and O_2 concentration for a $CdCr_2O_4$-attached device in the absence (○) or presence of 200 ppm NO (△) or 80 ppm NO_2 (□) at 550 °C

relation in the presence of 80 ppm NO_2 or 200 ppm NO. It should be noted that, in these measurements, the value of E_{EMF} obtained includes a contribution arising from the oxygen concentration cell formed between the sensing electrode and counter-electrode. This contribution can be measured separately under NO_x-free conditions as shown in the figure. The contribution of the mixed potential in these cases can be estimated as an increment of the E_{EMF} value in the presence of NO_x from the E_{EMF} value in the NO_x-free atmosphere. The data thus estimated are replotted in Fig. 8. The linear correlations have negative [-26 mV (decade)$^{-1}$] and small positive [1.3 mV (decade)$^{-1}$] slopes with increasing oxygen concentration at fixed concentrations of NO_2 and NO, respectively, consistent with theory ($-nA_1$ and $+pA_2$) from eqn. (V) and (XII).

Experimental evaluation of mixed potential

In order to confirm the sensing mechanisms proposed above, polarization curves of the $CdCr_2O_4$-attached device were measured in air and NO- or NO_2-containing air at 550 °C. As shown in Fig. 9, polarization curves shifted upward or downward, respectively, from that in air when the NO or NO_2 concentration in air was increased. These shifts of polarization curves are considered to appear because the electrochemical reaction of NO_2 [eqn. (2)] or NO [eqn. (5)] takes place in addition to that of oxygen [eqn. (3) or (4)]. It was assumed therefore that these shifts or the increments of electric current at each electrode potential were ascribed to the electric currents due to reaction (2) or (5).

Modified polarization curves ascribable to eqn. (2) or (5) were deduced in this manner and are replotted in Fig. 10, together with those for eqn. (3) and (4). In this figure, the electric currents in the anodic (for NO_2) or cathodic (for NO) polarization range are shown in absolute values for the sake of convenience in estimating the mixed potentials. For 80 ppm NO_2 in air, for example, the cathodic polarization curve for eqn. (2) intersects with the anodic polarization curve for eqn. (3) at an electrode potential of 27 mV, indicating that this value should be the mixed potential under this condition. The mixed potential values thus estimated are compared with the E_{EMF} values experimentally observed for the same concentrations of NO_2 and NO. Both values in each case are close to each other, supporting the sensing mechanisms involving the mixed potentials proposed above.

It is obvious from Fig. 10 that the mixed potential increases as the electrochemical reactions of NO_x [eqn. (2) and (5)], take place more actively relative to those of O_2. It follows that the excellent sensing properties of $CdCr_2O_4$ originate from the high electrode activity towards NO_x. The contribution of the Pt electrode has been ignored in the above; its contribution, if any, will be verified in future studies.

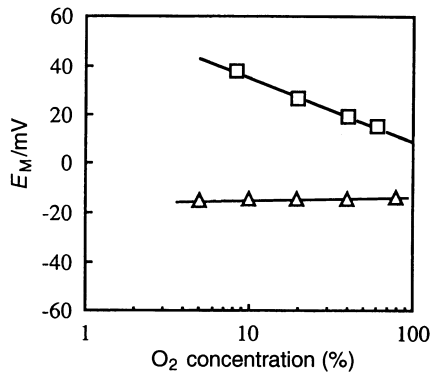

Fig. 8 Mixed potential *vs.* O_2 concentration correlation as estimated from Fig. 7

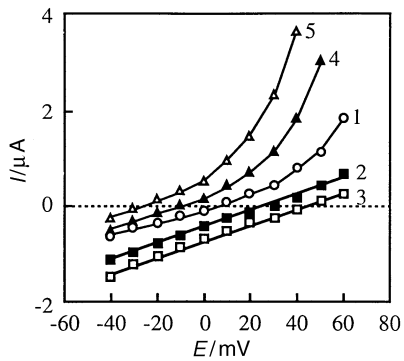

Fig. 9 Polarization curves of a $CdCr_2O_4$-attached device in various atmospheres at 550 °C: 1, air (○); 2, air + 80 ppm NO_2 (■); 3, air + 200 ppm NO_2 (□); 4, air + 200 ppm NO (▲); 5, air + 600 ppm NO (△)

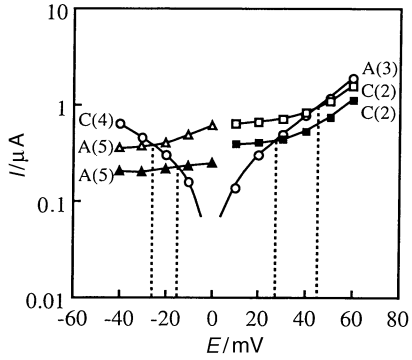

Fig. 10 Breakdown of the polarization curves in Fig. 9 into a couple of anodic (A) (O_2) and cathodic (C) (NO_2) currents ($E > 0$) or a couple of cathodic (O_2) and anodic (NO) currents ($E < 0$). The numbers in parentheses indicate the equations cited in the text. ○, Air; ■, NO_2 (80 ppm); □, NO_2 (200 ppm); ▲, NO (200 ppm); △, NO (600 ppm).

Conclusions

Electrochemical devices comprising of stabilized zirconia and spinel-type oxide electrodes were found to operate as solid-state NO or NO_2 sensors at high temperatures. A $CdCr_2O_4$-attached device gave the best sensing properties at 500–600 °C. Sensing mechanisms involving mixed potentials were supported from measurements of polarization curves.

This work was partially supported by Grant-in-Aid for Scientific Research from The Ministry of Education, Science, Sports and Culture of Japan, and a grant from the Steel Industry Foundation for the Advancement of Environmental Protection Technology.

References

1 M. Akiyama, J. Tamaki, N. Miura and N. Yamazoe, *Chem. Lett.*, 1991, 1611.
2 D. J. Smith, J. F. Vetelino, R. S. Falconer and E. L. Wittman, *Sens. Actuators B*, 1993, **13/14**, 264.
3 C. Cantalini, H. T. Sun, M. Faccio, M. Pelino, S. Santucci, L. Lozzi and M. Passacantando, *Sens. Actuators B*, 1996, **31**, 81.
4 G. Hotzel and W. Weppner, *Sens. Actuators*, 1987, **12**, 449.
5 N. Miura, S. Yao, Y. Shmizu and N. Yamazoe, *Sens. Actuators B*, 1993, **13/14**, 387.
6 N. Miura, S. Yao, Y. Shimizu and N. Yamazoe, *Solid State Ionics*, 1994, **70/71**, 572.
7 N. Miura, M. Iio, G. Lu and N. Yamazoe, *J. Electrochem. Soc.*, 1996, **143**, L241.
8 N. Miura, M. Iio, G. Lu and N. Yamazoe, *Sens. Actuators B*, **35/36**, 124.

9 N. Miura, Y. Yan, G. Lu and N. Yamazoe, *Sens. Actuators B*, 1996, **34**, 367.
10 N. Miura, G. Lu, N. Yamazoe, H. Kurosawa and M. Hasei, *J. Electrochem. Soc*., 1996, **143**, L33.
11 N. Miura, H. Kurosawa, M. Hasei, G. Lu and N. Yamazoe, *Solid State Ionics*, 1996, **86–88**, 1069.
12 G. Lu, N. Miura and N. Yamazoe, *J. Electrochem. Soc*., 1996, **143**, L154.
13 G. Lu, N. Miura and N. Yamazoe, *Sens. Actuators B*, 1996, **35/36**, 130.

Paper 7/01708A; *Received* 11*th March*, 1997